

Nonparametric determination of redshift evolution index of Dark Energy

Houri Ziaeepour

Mullard Space Science Laboratory, Holmbury St. Mary, Dorking, Surrey, RH5 6NT, UK.

E-mail: hz@mssl.ucl.ac.uk

Abstract. We propose a nonparametric method to determine the sign of γ - the redshift evolution index of dark energy. This is important for distinguishing between positive energy models, a cosmological constant, and what is generally called ghost models. Our method is based on geometrical properties and is more tolerant to uncertainties of other cosmological parameters than fitting methods in what concerns the sign of γ . The same parameterization can also be used for determining γ and its redshift dependence by fitting. We apply this method to SNLS supernovae and to gold sample of re-analyzed supernovae data from Riess *et al.* 2004. Both datasets show strong indication of a negative γ . If this result is confirmed by more extended and precise data, many of dark energy models, including simple cosmological constant, standard quintessence models without interaction between quintessence scalar field(s) and matter, and scaling models are ruled out.

Recent observations of Supernovae (SNe), Cosmic Microwave Background (CMB), and Large Scale Structures (LSS) indicate that the dominant content of the Universe is a mysterious energy with an equation of state very close to Einstein cosmological constant. The equation of state is defined by w , the ratio of pressure p to density ρ , $w = P/\rho$. For a cosmological constant $w = -1$. The observed mean value of w for dark energy is very close to -1 . Some of the most recent estimations of w are: From combination of 3-year WMAP and SuperNova Legacy Survey (SNLS), $w = -0.97_{0.09}^{+0.07}$ [2]; from combination of 3-year WMAP, large scale structure and supernova data, $w = -1.06_{-0.009}^{+0.016}$ [2]; from combination of CMAGIC supernovae analysis and baryon acoustic peak in SDSS galaxy clustering statistics at $z = 0.35$, $w = -1.21_{-0.12}^{+0.15}$ [3]; and finally from baryon acoustic peak alone $w = -0.8 \pm 0.18$. It is evident that with inclusion of one or two sigma uncertainties to measured mean values, the range of possible values for w runs across the critical value of -1 . Moreover, in all these measurements the value of w depends on other cosmological parameters and their uncertainties in a complex way. Reconstruction methods for determining cosmological parameters from observations - see [4] and references therein for a review of methods - usually use fitting of continuous parameters on the data and determine a range for w . On the other hand, the sign of $w + 1$ is more crucial for distinguishing between various dark energy models than its absolute value. For instance, if $w + 1 < 0$, quintessence models with conventional kinetic energy and potential are ruled out because in these models this quantity is always positive. Decay of dark matter to dark energy or an interaction between these components can lead to an effective $w + 1 < 0$ without violating null energy condition[8]. Redshift dependence of w has been invoked in many of recent works. Although the quality of available data does not yet permit to obtain a precise measurement of variability of w , recent attempts show that at low redshifts this can not be very large [7], see also the results of present work below.

Without loss generality the density of the Universe at redshift z can be written in the following form:

$$\frac{\rho(z)}{\rho_0} = \Omega_m(1+z)^3 + \Omega_h(1+z)^4 + \Omega_{de}(1+z)^{3\gamma} \quad (1)$$

where $\rho(z)$ and ρ_0 are total density at redshift z and in local Universe, respectively; Ω_m , Ω_h , and Ω_{de} are respectively cold and hot matter, and dark energy fraction in the total density at $z = 0$. We consider a flat universe in accordance with recent observations[2]. At low redshifts, the contribution of the CMB to the total mass of the Universe is negligible. The contribution of neutrinos is $\Omega_\nu h^2 = \sum m_\nu / 92.8 \text{ eV}$, $h \equiv H_0 / 100 \text{ km Mpc}^{-1} \text{ sec}^{-1}$, where H_0 is present Hubble constant. The upper limit on the sum of the mass of neutrinos from 3-year WMAP is $\sum m_\nu < 0.62$ (95% confidence level)[11]. Even if one of the neutrinos has very small mass and behaves as a warm dark matter, for $z < 1$ neutrino contribution to the total mass is $\lesssim 4\%$, smaller than the uncertainty on dark matter contribution. Thus, the approximation $\Omega_m + \Omega_{de} \approx 1$ is justified.

Here we propose a nonparametric method specially suitable for estimating the sign

of γ . When the quality of data is adequate, the quantity $A(z)$ defined in (3) can also be used to fit the data and to measure the value of γ . The expression *nonparametric* here is borrowed from signal processing literature where it means testing a null hypothesis against an alternative hypothesis by using a discrete condition such as jump, sign changing, etc., in contrast to constraining a continuous parameter (see e.g. [9]). We show that geometrical properties of $A(z)$ are related to the sign of γ and we can detect sign without fitting a continuous parameter.

Assuming a constant w

$$\gamma = w + 1 \quad (2)$$

and it can be easily shown that in this case:

$$\mathcal{A}(z) \equiv \frac{1}{3(1+z)^2 \rho_0} \frac{d\rho}{dz} - \Omega_m = \gamma \Omega_{de} (1+z)^{3(\gamma-1)} \quad (3)$$

If the equation of state of dark energy varies with redshift, we can assume that γ in (1) depends on redshift. In this definition γ is related to the equation of state of dark energy according to:

$$\gamma(z) = \frac{1}{\ln(1+z)} \int_0^z dz' \frac{1+w(z')}{1+z'} \quad (4)$$

and:

$$A(z) = \Omega_{de} \left(\gamma(z) + (1+z) \ln(1+z) \frac{d\gamma}{dz} \right) (1+z)^{3(\gamma-1)} \quad (5)$$

When w is constant (4) and (5) approach respectively to (2) and (3). If $w(z)$ is a slowly varying function of redshift, we can parameterize it as:

$$w(z) = w_0 + w_1 z \quad (6)$$

where w_0 and w_1 are constant, and $|w_1/w_0| < 1$. This leads to:

$$\gamma(z) = 1 + w_0 + w_1(z/\ln(1+z) - 1) \quad (7)$$

By expanding the logarithm term at low redshifts it is straightforward to see that at lowest order $\gamma \approx 1 + w_0 + w_1 z/2$. Therefore $\gamma(z)$ varies even more slowly than w . Using (7) and (5), we can find the explicit expression of $A(z)$ as a function of constant parameters:

$$\begin{aligned} A(z) &= \Omega_{de} \left(\gamma(z) + \frac{w_1[(1+z)\ln(1+z) - z]}{\ln(1+z)} \right) (1+z)^{3(\gamma-1)} \\ &\approx \Omega_{de} \left(\gamma(z) + w_1 \left(\frac{z^2}{2} + \dots \right) \right) (1+z)^{3(\gamma-1)} \end{aligned} \quad (8)$$

This shows that at low redshifts the contribution of derivative term is quadratic in z and negligible in comparison with $\gamma(z)$. Therefore, at low redshifts the sign of $A(z)$ follows the sign of $\gamma(z)$ even for a redshift-dependent equation of state. On the other hand, for $z < 1$ this parameterization is equivalent to models IV and IV of Serra *et al.* [7], which are barely constrained and are consistent with zero or small w_1 . This confirms that the assumption of a constant or slowly varying γ at low redshifts in (3) is a valid

approximation for our Universe. Therefore in this work from now on we consider only this case, unless the redshift dependence of γ is explicitly mentioned.

Similar expressions can be obtained for non-standard cosmologies such as DGP[12] model and other string/brane inspired cosmologies [13]. It is also possible to find an expression similar to (3) for non-flat FLRW models and without neglecting hot matter. The left hand side would however depend on Ω_k and Ω_h , and therefore would be more complex. Nonetheless, when their contribution at low redshifts are much smaller than cold matter and dark energy, the general behaviour of $\mathcal{A}(z)$ will be the same as approximate case studied here.

In summary, the right hand side of (3) has the same sign as γ if $|\gamma(z)| \gg (1+z)\ln(1+z)|\gamma'(z)|$. Moreover, the sign of $\mathcal{A}(z)$ derivative is opposite to the sign of γ because due to the smallness of observed γ , the term $\gamma - 1$ is negative (if γ depends on z this is true only for low redshifts). This means that $\mathcal{A}(z)$ is a concave or convex function of redshift, respectively for positive or negative γ . In the case of a cosmological constant $\mathcal{A}(z) = 0$ for all redshifts. This second feature of expression (3) is interesting because if Ω_m is not correctly estimated, $\mathcal{A}(z)$ will be shifted by a constant, but its geometrical properties will be preserved.

The left hand side of expression (3) can be directly estimated from observations. More specifically, Ω_m is determined from conjunction of CMB, LSS, and supernova type Ia data, and at present it is believed to be known with a precision of $\sim 5\%$. At low redshifts, the derivative of the density is best estimated from SN type Ia observations. In the case of FLRW cosmologies, the density and its derivative can be related to luminosity distance D_l , and its first and second derivatives:

$$\mathcal{B}(z) \equiv \frac{1}{3(1+z)^2\rho_0} \frac{d\rho}{dz} = \frac{\frac{2}{1+z} \left(\frac{dD_l}{dz} - \frac{D_l}{1+z} \right) - \frac{d^2D_l}{dz^2}}{\frac{3}{2} \left(\frac{dD_l}{dz} - \frac{D_l}{1+z} \right)^3} \quad (9)$$

$$D_l = (1+z)H_0 \int_0^z \frac{dz}{H(z)} \quad , \quad H^2(z) = \frac{8\pi G}{3} \rho(z) \quad (10)$$

It is remarkable that the right hand side of (9) depends only on one cosmological parameter, H_0 . Moreover, similar to an uncertainty on Ω_m , H_0 uncertainty rescales $\mathcal{B}(z)$ similarly at all redshifts, but does not modify geometrical properties $\mathcal{B}(z)$ and $\mathcal{A}(z)$. D_l can be directly obtained from observed luminosity of standard candles such as supernovae type Ia. In the case of LSS observations where the measured quantity is the evolution of ρ with redshift, $\mathcal{B}(z)$ is measured directly up to an overall scaling by ρ_0 . This does not change the geometrical properties of $\mathcal{B}(z)$ and $\mathcal{A}(z)$ either. The scaling by a positive constant does not flip a convex curve to concave or vis-versa. In summary, uncertainties of Ω_m and H_0 do not affect the detection of the sign of γ through geometrical properties of $\mathcal{A}(z)$. This is quite different from fitting methods. They are sensitive to all numerical parameters H_0 , Ω_m , Ω_{de} , and w in a complex way, usually through a non-linear equation such as chi-square or likelihood. This makes the assessment of the influence of uncertainties on parameter estimation, and specifically on the determination of the sign of γ very difficult.

When this method is applied to standard candle data such as supernovae type Ia, one has to calculate first and second derivatives of D_l . Numerical calculation of derivatives is not however trivial. To have a stable and enough precise result, not only the data must have high resolution and small scatter, but also it is necessary to smooth it. Therefore, to test the stability of numerical calculations and the method in general, we also apply it to simulated data. The details of numerical methods is discussed in the Appendix.

Examples of reconstruction of simulated data are shown in Fig.1. It is evident that despite deformation of the reconstructed curves due to numerical errors and uncertainties, specially close to lower and upper redshift limits, the difference between convexity of curves for positive and negative γ is mostly preserved and can be used, either by visual inspection or by using a slope detection algorithm, to find the sign of γ . The simulated data is however much more uniform - has less scatter - than presently available data, see Fig.1. Therefore the reconstruction from real data is more prone to artifacts than simulated ones. Fig.1 shows that although at mid-range redshifts the data follow a curve similar to what is expected from FLRW cosmologies, deviations appear close to boundaries and at high redshifts where the quality of data is worse. We attribute these to the artifacts of reconstructions.

Visual inspections or slope detection lack a quantitative estimation of uncertainties of the measured sign for γ . In signal processing usually binomial estimation of the probability or optimization of detection[10] is used to assess uncertainties. However, in most practically interesting contexts in signal processing, the signal is constant and uncertainties are due to noisy. In the cosmological sign detection discussed here the observable $\mathcal{A}(z)$ is both noisy and varies with redshift. Therefore, binomial probability and similar methods are not applicable. For this reason we try another strategy, specially suitable for this cosmological sign detection task.

The null hypothesis for dark energy is $\gamma = 0$. Assuming a Gaussian distribution for the uncertainty of reconstructed $\mathcal{A}(z)$ from data and from simulated data with $\gamma = 0$, for each data-point we calculate the probability that the data-point belongs to the null hypothesis. To include the uncertainty of data, we integrate the uncertainty distribution 1-sigma around the mean value:

$$P_i = \frac{1}{\sqrt{2\pi(\sigma_{0i}^2 + \sigma_i^2)}} \int_{\mathcal{A}_i - \sigma_i}^{\mathcal{A}_i + \sigma_i} dx e^{-\frac{(x - \mathcal{A}_{0i})^2}{2(\sigma_{0i}^2 + \sigma_i^2)}} \quad (11)$$

where \mathcal{A}_i and σ_i belong to the i^{th} data-point, and \mathcal{A}_{0i} and σ_{0i} belong to simulated null hypothesis model at the same redshift. Averaging over P_i gives \bar{P} , an overall probability that the dataset corresponds to the null hypothesis. As $\gamma = 0$ is the limit case for $\gamma > 0$, \bar{P} is also the maximum probability of $\gamma > 0$.

We have applied this algorithm to two supernova datasets: published data from SuperNova Legacy Survey (SNLS)[5], and to supernovae with $z < 0.45$ from gold sample of re-analyzed data by Riess *et al.*2004[1]. The reason for using only the low redshift subset of the latter compilation is that scatter and uncertainties of the peak magnitude

at higher redshifts is too large and reconstructed $\mathcal{A}(z)$ is instable. Fig.1 shows $\mathcal{A}(z)$ obtained from these data as well as from simulated SNe as described in the caption. Simulated standard sources are put at the same redshifts as real data to make simulated samples as similar to data as possible. In both datasets the probability of $\gamma \lesssim 0$ or equivalently $w \lesssim -1$ is larger than 70%. The SNLS data is consistent with a γ as small as ~ -0.2 [‡]. There is however significant deviation from a smooth distribution for $z \lesssim 0.1$ and $z \gtrsim 0.5$. We attribute this to large scatter of the data at these redshifts see Fig.2-a. The fact that at intermediate redshifts in these datasets $\mathcal{A}(z)$ follows closely models with constant γ is a demonstration of very small variation of γ in these redshifts, consistent with our arguments above.

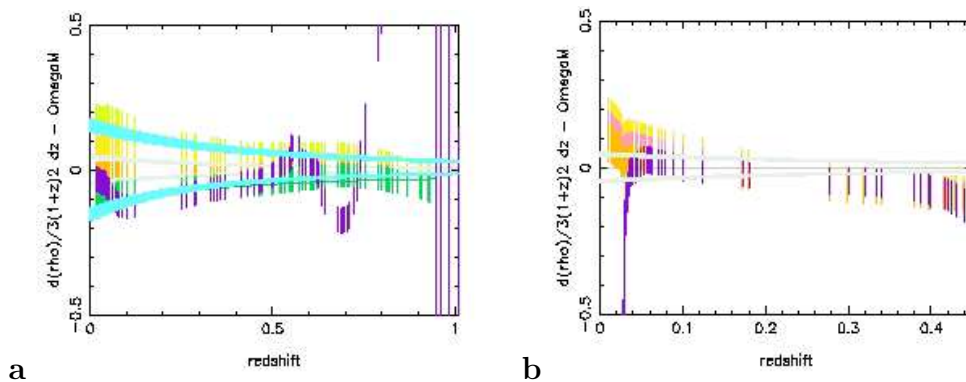


Figure 1. $\mathcal{A}(z)$ from 117 SNe of the SNLS (**a**-purple curve), and from 88 SNe with $z < 0.45$ recompiled and re-analyzed by Riess *et al.*2004[1] (**b**-purple curve). Error bars are 1-sigma uncertainty. In (**a**), green, orange, yellow, and light green curves are the reconstruction of $\mathcal{A}(z)$ from simulations for $\gamma = -0.2, -0.06, 0.6, 0.2$, respectively. The probability of null hypothesis ($\gamma = 0$) is $\bar{P} = 0.27$, therefore the probability of $\gamma < 0$, $1 - \bar{P} = 0.73$. Light grey and cyan curves are theoretical calculation including the uncertainty on Ω_{de} , respectively for $\gamma = \pm 0.06, \pm 0.2$. In (**b**), the pink curve is simulated $\gamma = 0$ model. For this dataset $1 - \bar{P} = 0.75$. The dark grey straight line is the theoretical expectation for $\mathcal{A}(z)$ when dark energy is a cosmological constant. For all models $H_0 = 73 \text{ km Mpc}^{-1} \text{ sec}^{-1}$ and $\Omega_{de} = 0.77$.

To see whether the large negative γ concluded from the SNLS data is due to scattering and/or reconstruction artifacts, we also apply the same formalism to a subset of these data with $z < 0.45$. The result is shown in Fig.2-b along with simulations in the same redshift range. The *bump* at very low redshifts in Fig.1 does not exist in this plot, and therefore we conclude that it has been an artifact of numerical reconstruction. Although $\mathcal{A}(z)$ distribution in this dataset is also convex and the probability of $\gamma < 0$ is larger than 90%, it does not have the same slope as any of constant w models. It seems that low and high redshift sections of the curve correspond to different values of γ . For $z \lesssim 0.15$, $\mathcal{A}(z)$ is close to theoretical and simulated data with $\gamma = -0.2$. For $z \gtrsim 0.25$, $\mathcal{A}(z)$ approaches the values for larger and even positive γ . Such behaviour

[‡] Here we concentrate on the sign of γ and don't perform any fitting to obtain its value. Estimations are from comparison with simulations.

does not appear in Fig.1. Giving the fact that the number of available data points with $z \gtrsim 0.25$ in this subset is small, the most plausible explanation is simply numerical artifacts. Alternative explanations are the evolution of γ with redshift or the use of under-estimated value for Ω_m . If the latter case is true, the value of γ must be even smaller than -0.2 . Interestingly, the deviation from a constant w model in the former case is consistent, up to uncertainties, with the best estimations of the evolution of w in models IV and VI of Ref. [7]. This confirms the consistency of two reconstruction and parameter estimation methods. However, as explain above, present method shows that this deviation can be also due to uncertainties of Ω_m and not the evolution of w . The simplicity of dependence on the cosmological parameters in this method permits to see their effects more explicitly than in fits. With a data gap in $0.15 \lesssim z \lesssim 0.25$ interval and only 58 supernovae in this subset, it is not possible to make any definite conclusion about the behaviour of this data. We should also mention that SNLS supernovae with $z < 0.25$, and at $0.25 < z < 0.4$, and $z > 0.4$ have not been treated in the same way[5]. It is therefore possible that some of the observed features are purely artifacts of the analysis of the raw observations.

Fig.1-**b** shows $\mathcal{A}(z)$ from gold SNe sample recompiled by Riess, *et al.*[1]. It is also consistent with $\gamma < 0$ with a probability $\sim 75\%$ at 1-sigma and $\sim 66\%$ at 2-sigma. This plot shows that the value of γ estimated from this data is ~ -0.06 , larger than estimation from SNLS data.

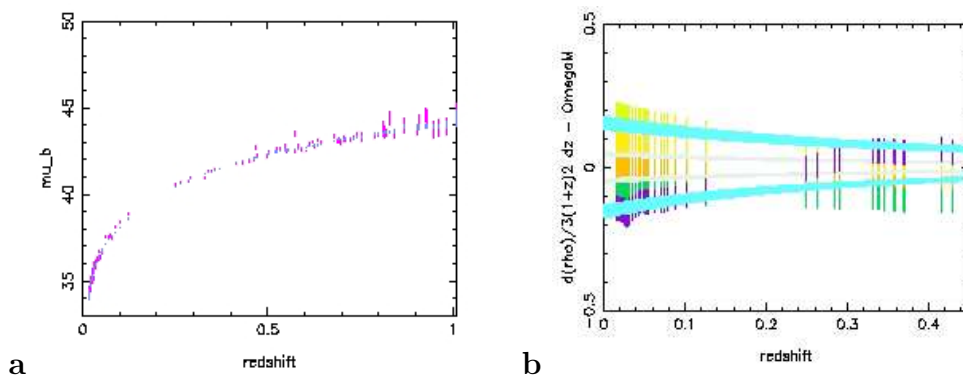


Figure 2. **a:** μ_b from SNLS supernovae, data (magenta), smoothed distribution (blue). Although this distribution look quite smooth, even small sudden variations can lead to large variations in derivatives. **b:** $\mathcal{A}(z)$ for SNLS supernovae with $z < 0.45$. Definition of curves is the same as in Fig.1. For this dataset $1 - \bar{P} = 0.93$ when cosmological parameters are the same as Fig.1. If $\Omega_{de} = 0.73$ is used, $1 - \bar{P} = 0.96$.

The reason for the difference between estimated values for γ from SNLS and Riess, *et al.* compilation here is not clear because value of w reported in Ref.[1] and Ref[5] are consistent. Nonetheless, the estimated values are in the range reported by other works[2][3]. Most probably this difference is related to different scatter and uncertainty of these datasets, and the fact that low and high redshift data are not treated in the same way. Recent claims about contamination of supernova type Ic and the effect of

asymmetric explosion in the lightcurve of supernova type Ia[14], and possible differences between low and high redshift supernovae[15] can not explain the differences either, because they affect both surveys in the same way. Despite these discrepancies, both datasets are in good agreement about negative sign of γ .

These results highlight various shortcomings in both datasets used here. Our first remark is the large gap in redshift distribution of observed supernovae in redshift range $0.1 \lesssim z \lesssim 0.3$. Both datasets have less than 6 supernovae in this range and nothing in $0.15 \lesssim z \lesssim 0.25$. This is not an important issue for finding redshift distribution of D_l , but redshift gap becomes very important when derivatives of D_l are calculated. The lack or rareness of supernovae data in this redshift range is related partly to the history of star formation in galaxies[16], and partly to optimization of surveys[17] for detection of very low or high redshift supernovae which decreases the probability of detection of mid-range SNe. Sloan Supernova Survey[18] is optimized to detect SNe in $0.1 \lesssim z \lesssim 0.35$ and should provide the missing data in near future.

Our second observation is a large scatter in both datasets around redshift ~ 0.55 , see Fig.2-a. This leads to a large scatter in the numerical determination of derivatives in (9) and makes the results unusable. In future observations the reason of this large scatter should be understood.

From theoretical calculation and simulations shown in Fig.1 one can also conclude that with present uncertainties of cosmological parameters, the most important redshift range for determining the equation of state of dark energy is $z \lesssim 0.8$. Higher redshift supernovae are only interesting if w varies significantly with redshift. Although technical challenges, understanding of physics of supernovae and their evolution[15], and applications for other astronomical ends make the search of supernovae at larger distances interesting, they will not be in much use for determining the equation of state of dark energy, at least not at the lowest level which is the determination of redshift independent component of w .

On the other hand, improvements in numerical techniques and algorithms would lead to better measurements. One of the possibilities in this direction is the application of an adaptive smoothing algorithm with variable degrees of smoothing depending on the amount of scatter in the data. More sophisticated smoothing algorithms also have been proposed[19]. We postpone the application of these advanced methods to future, when larger datasets become available.

In summary, we have proposed a nonparametric formalism to investigate the sign of γ in the equation of state of dark energy. When data with better quality become available, fitting can be added to this method to find also the value of γ . The advantage of this method is its geometrical nature when the sign of γ is searched. Moreover, its simple dependence on cosmological parameters makes the assessment of uncertainties of the value of γ easier. This method is suitable for applying to observations in which the total density of the Universe and its variation are directly measured such as standard candles and galaxy surveys, but not to integrated observables such as CMB anisotropy. By applying this method to two of largest publicly available supernovae datasets we

showed that they are consistent with a $w < -1$. Present data is not however enough precise to permit the estimation of $|w + 1|$ with good certainty. With on-going projects such as SNLS, Supernova Cosmology Project[20], and SDSS SNe survey, and future projects such as SNAP and DUNE, enough precise datasets should be available soon.

Appendix: For standard candles, $\mathcal{A}(z)$ must be calculated from luminosity distance which is related to magnitude: $D_l/D_0 = 10^{\mu_b/5}$. D_0 is the distance for which the common luminosity of standards is determined and depends on H_0 . Therefore, μ_b needs a correction if a different H_0 is used[5]. For simulated data, D_l is calculated from (10) and μ_b is determined from definition above, then a random noise with a standard deviation of 3% is added to the magnitude.

Expression (9) for $\mathcal{B}(z)$ contains the first and the second derivatives of D_l which must be calculated numerically from data. It is however well known that a direct determination of derivatives leads to large and unacceptable deviation from exact values. One of the most popular alternatives is fitting a polynomial around each data point and then calculating an analytical derivative using the polynomial approximation in place of the data. We use this approach to determine derivatives of μ_b and D_l . In addition, before applying this approach, we smooth the distribution of magnitudes using again the same polynomial fitting algorithm. In FLRW cosmologies the redshift evolution of the luminosity distance is very smooth. Therefore, a second order polynomial for smoothing is adequate. Fitting is based on a right-left symmetric, least χ^2 algorithm, and for this we have implemented *lfit* function of Numerical Recipes[21]. By trial and error we find that 19 data-point fitting gives the most optimal results regarding the number of available data points and their scatter. Close to boundaries however less data point for fitting is available in one side of each point, and therefore the fitting is less precise. The artifacts discussed above are mostly related to this imprecision of calculation near boundaries. In the present work no adaptive smoothing is applied. In addition to smoothed data and their derivatives, the function *lfit* calculates a covariant matrix for uncertainties of parameters (derivatives). We use diagonal elements as 1-sigma uncertainty of the smoothed data and its derivatives. The uncertainty of $\mathcal{A}(z)$ is calculated from the uncertainty of terms in (3) and (9) using error propagation relation: For $f(x_1, x_2, \dots)$, $\sigma_f^2 = \sum_i \sigma_{x_i}^2 (\partial f / \partial x_i)^2$. Smoothed terms and parameters in $\mathcal{A}(z)$ are considered as independent variables with their own uncertainty.

- [1] A.G. Riess, *et al.*, *ApJ.* **607**, (2004) 665, astro-ph/0402512.
- [2] Spergel, D.N. *et al.*, astro-ph/0603449.
- [3] A. Conley, *et al.*, *ApJ.* **644**, (2006) 1, astro-ph/0602411.
- [4] V. Sahni, A. Strarobinsky, astro-ph/0610026.
- [5] P. Astier, *et al.*, *A.& A.* **447**, (2006) 31, astro-ph/0510447.
- [6] D.J. Eisenstein, *et al.*, *ApJ.* **633**, (2005) 560, astro-ph/0501171.
- [7] P. Serra, A. Heavens & A. Melchiorri, astro-ph/0701338.
- [8] H. Ziaepour, astro-ph/0002400, H. Ziaepour, *Phys. Rev. D* **69**, (2004) 063512, astro-ph/0308515, S. Das, P.S. Corasaniti, J. Khoury, *Phys. Rev. D* **73**, (2006) 083509, astro-ph/0510628, H. Ziaepour, hep-ph/0603125.
- [9] E.L. Lehmann, H.J.M. Dabrera, *Nonparametrics*, Holden-Day, San Fransisco, CA, 1975, J.M. Moriss, *IEEE Trans. Comm.* **39**, (1991) 1726.

- [10] H. Gil Kim, *et al.*, IEEE MILCOM 97 Proceedings, Vol. 3, (1997), 1382.
- [11] S.Hannestad, G.G. Raffelt, astro-ph/0607101.
- [12] G. Dvali, G. Gabadadze & M. Porrati, *Phys. Lett. B* **484**, (2000) 112 hep-th/0002190, *Phys. Lett. B* **484**, (2000) 129, hep-th/0003054, *Phys. Lett. B* **485**, (2000) 208, hep-th/0005016.
- [13] P. Kanti, K.A. Olive & M. Pospelov, PRD **62**, (2000) 126004, hep-ph/0005146, P. Binétury, C. Deffayet & D. Langlois, *Nucl. Phys. B* **565**, (2000) 269, hep-th/9905012, P. Kanti, I.I., Kogan I.I., K.A. Olive & M. Pospelov, *Phys. Lett. B* **468**, (1999) 31, hep-ph/9909481, *Phys. Rev. D* **61**, (2000) 106004, hep-ph/9912266; C. Csaki *et al.*, *Phys. Rev. D* **62**, (045015) 2000, hep-ph/9911406, H. Ziaepour, hep-ph/0010180 (examples of early works).
- [14] J. Middleditch, astro-ph/0608386.
- [15] A.G. Riess, M. Livio, astro-ph/0601319.
- [16] A. Gal-Yam, D. Maoz, *MNRAS* **347**, (2004) 942, astro-ph/0309796.
- [17] F. Simpo, S. Bridle, *Phys. Rev. D* **73**, (2006) 083001, astro-ph/0602213.
- [18] M. Sako, *et al.*, astro-ph/0504455.
- [19] A. Shafieloo, *et al.*, *MNRAS* **366**, (2006) 1081, astro-ph/0505329.
- [20] A.R. Knop *et al.*, *ApJ*. **598**, (2003) 102, astro-ph/0309368.
- [21] W.H. Press, *et al.*, “Numerical Recipes in C”, Cambridge University Press.